
1 Van Allen Probes observation of plasmaspheric 2 hiss modulated by injected energetic electrons

3 Run Shi¹, Wen Li¹, Qianli Ma^{2,1}, Seth G. Claudepierre³, Craig A. Kletzing⁴, William S.
4 Kurth⁴, George B. Hospodarsky⁴, Harlan E. Spence⁵, Geoff D. Reeves⁶, Joseph F. Fennell³,
5 J. Bernard. Blake³, Scott A. Thaller⁷, and John R. Wygant⁷

6

7 ¹Center for Space Physics, Boston University, Boston, Massachusetts, USA.

8 ²Department of Atmospheric and Oceanic Sciences, University of California, Los Angeles,
9 Los Angeles, California, USA.

10 ³Space Science Department, The Aerospace Corporation, El Segundo, California, USA.

11 ⁴Department of Physics and Astronomy, University of Iowa, Iowa City, Iowa, USA.

12 ⁵Institute for the Study of Earth, Oceans, and Space, University of New Hampshire,
13 Durham, New Hampshire, USA.

14 ⁶Space Science and Applications Group, Los Alamos National Laboratory, Los Alamos,
15 New Mexico, USA.

16 ⁷School of Physics and Astronomy, University of Minnesota, Twin Cities, Minneapolis,
17 Minnesota, USA.

18

19

20 Corresponding author:

21 Run Shi

22 Center for Space Physics, Boston University, Boston, Massachusetts, USA

23 runs@bu.edu

24

25 **Key points**

26 1. Clear evidence is provided for local amplification of plasmaspheric hiss by anisotropic

27 electron distributions

28 2. Hiss wave intensity variation is well correlated with injected electron flux modulation

29 3. The modulation of injected electron fluxes is correlated with ULF wave fluctuations

30

Abstract

Plasmaspheric hiss was observed by Van Allen Probe B in association with energetic electron injections in the outer plasmasphere. The energy of injected electrons coincides with the minimum resonant energy calculated for the observed hiss wave frequency. Interestingly, the variations of hiss wave intensity, electron flux, and ULF wave intensity exhibit remarkable correlations, while plasma density is not correlated with any of these parameters. Our study provides direct evidence for the first time that the injected anisotropic electron population, which is modulated by ULF waves, modulates the hiss intensity in the outer plasmasphere. This also implies that plasmaspheric hiss observed by Van Allen Probe B in the outer plasmasphere ($L > \sim 5.5$) is locally amplified. Meanwhile, Van Allen Probe A observed hiss emission at lower L shells (< 5), which was not associated with electron injections but primarily modulated by the plasma density. The features observed by Van Allen Probe A suggest that the observed hiss deep inside the plasmasphere may have propagated from higher L shells.

1. Introduction

Plasmaspheric hiss plays an important role in the loss of energetic electrons within the plasmasphere and in high-density plumes [Lyons *et al.*, 1972; Lyons and Thorne, 1973; Albert, 2005; Meredith *et al.*, 2007, 2009; Summers *et al.*, 2008; Ni *et al.*, 2013; Breneman *et al.*, 2015; Li *et al.*, 2015a; Ma *et al.*, 2016]. However, the generation mechanisms of plasmaspheric hiss remain under active research. Three mechanisms have received the

most intense attention to explain the generation of plasmaspheric hiss, including in situ growth of waves [Thorne *et al.*, 1979; Church and Thorne, 1983], lightning generated whistlers [Green *et al.*, 2005], and whistler mode chorus waves as an “embryonic source” [Bortnik *et al.* 2008, 2009; Chen *et al.* 2012a, 2012b]. Although wave power above 2–3 kHz from lightning-generated whistlers shows some correlation with hiss waves [Green *et al.*, 2005], the waves below 1 kHz, which contain the majority of hiss wave power, are independent of lightning flash rate [Meredith *et al.*, 2006]. The in situ growth of waves inside the plasmasphere was shown to be inadequate to account for the observational level (~ 20 dB) [Huang *et al.*, 1983]; in response, Church and Thorne [1983] suggested that an “embryonic source” is required to lead to the observed wave intensity. Recent studies based on ray tracing simulation [Bortnik *et al.*, 2008] have demonstrated that chorus waves from the distant magnetosphere can propagate into the plasmasphere and act as an embryonic source for the hiss wave generation. Furthermore, ray tracing simulations [Chen *et al.*, 2012a] suggested that the majority of hiss formation is caused by chorus emission originating within $\sim 3 R_E$ from the plasmopause. This model has successfully explained the observed frequency spectrum and spatial distribution of the observed hiss over the typical hiss frequency range from 100 Hz to several kHz. A number of observational studies [Bortnik *et al.*, 2009; Wang *et al.*, 2011; Meredith *et al.* 2013; Li *et al.*, 2015b] have shown good correlations between chorus and plasmaspheric hiss and suggested that chorus plays an important role in hiss wave intensification.

Van Allen Probes recently detected unusually low frequency hiss emissions with wave power extending well below 100 Hz [Li *et al.*, 2013]. The low frequency hiss was demonstrated to cause more efficient loss of high energy electrons (from ~50 keV to a few MeV) due to its stronger pitch angle scattering rates compared to normal hiss [Ni *et al.*, 2014; Li *et al.*, 2015a]. Such low frequency hiss is unlikely to be a result of propagation of chorus waves from a more distant region because embryonic chorus waves at the same frequency [Bortnik *et al.*, 2008] would need to originate from unrealistically high L shells [Li *et al.*, 2015b]. Therefore, these low frequency hiss waves were suggested to be generated in the outer plasmasphere on the dayside through local amplification [Li *et al.*, 2013; Chen *et al.*, 2014; Shi *et al.*, 2017].

Hiss intensity modulation is often driven by the variation of background plasma density either through local amplification or wave propagation [Chen *et al.*, 2012c], and the modulation of hiss by other factors may easily be suppressed by the effect of the plasma density. Therefore, observations showing direct correlation between hiss emission and electron flux are still very limited. In fact, electron fluxes of energetic electrons (tens to hundreds of keV) can be modulated by Ultra Low Frequency (ULF) waves. A typical modulation is caused by drift-resonance [Southwood and Kivelson, 1981]. Zong *et al.* [2009] showed an interesting event of energetic electron modulation by shock induced ULF waves. More recently, Claudepierre *et al.* [2013] presented observations of electron drift resonance with the fundamental poloidal mode of ULF waves based on Van Allen Probes measurements. The energy dependence of the amplitude and phase of the electron flux

modulations provided strong evidence for such an interaction. The peak electron flux modulations occurred over 5-6 wave cycles at energies ~ 60 keV. The drift-resonance between electrons and ULF waves has been extensively studied both theoretically and observationally based on Van Allen Probes data [Dai *et al.*, 2013; Hao *et al.*, 2014; Chen *et al.*, 2016; Zhou *et al.*, 2015, 2016; Li *et al.*, 2017]. Such modulation of energetic electrons may modulate hiss emissions by varying the electron flux and pitch angle anisotropy, which could potentially affect the local growth rates of hiss waves, but the observational evidence has not been reported yet. In this study, we report on a modulation of hiss wave intensity and injected electron flux due to ULF waves observed by Van Allen Probe B near the dayside, providing clear evidence that the hiss emission was generated through local amplification in the outer plasmasphere.

2. Data and Methodology

The Van Allen Probes comprise two identical spacecraft (Probes A and B) in near-equatorial orbits with an altitude of ~ 600 km at perigee and geocentric distance of $\sim 5.8 R_E$ at apogee [Mauk *et al.*, 2012]. The Electric and Magnetic Field Instrument Suite and Integrated Science (EMFISIS) suite on Van Allen Probes A and B includes a magnetometer and a Waves instrument [Kletzing *et al.*, 2013]. The DC magnetic field is measured by the magnetometer, and the survey mode of Waveform Receiver (WFR) provides the power spectral density from 10 Hz to 12 kHz at 6 s time resolution. Plasma density can be either calculated based on the upper hybrid resonance frequency extracted from the High

Frequency Receiver (HFR) data [Kurth *et al.*, 2015] or be inferred from the spacecraft potential measured by the Electric Field and Waves (EFW) instrument [Wygant *et al.*, 2013]. We inferred plasma density profiles based on the measurements from both instruments in the present study to obtain accurate plasma density values with high time resolution. High resolution electron flux measurements over the energy range of ~ 30 keV to 4 MeV are provided by the Magnetic Electron Ion Spectrometer (MagEIS) instrument [Blake *et al.*, 2013; Spence *et al.*, 2013]. We used the level 3 MagEIS dataset which includes particle pitch angle distribution in this study to evaluate the electron distribution responsible for the hiss wave generation.

3. Observational Results

A hiss intensification event modulated by electron injection was observed by Van Allen Probe B during ~ 20 -22 UT on 12 January 2014, as shown in Figure 1. The satellite was located on the dayside and remained inside the plasmasphere, indicated by the high plasma density (Figure 1f). The main power of the hiss emission (Figures 1b and 1c) resided below the lower hybrid resonance frequency (white dash-dotted line in Figure 1b) and 100 Hz (white dashed line in Figure 1c) and intensified following the increase in the AE index (Figure 1a). Figure 1e presents the magnitude of the background magnetic field. The spin averaged electron flux (Figure 1g) exhibited modulations with a period of about 6 minutes. There is also a variation in the electron pitch angle anisotropy (Figure 1h) although it is not as clear as the modulations of electron flux. The electron anisotropy is

calculated based on *Chen et al.* [1999]. The black lines in Figures 1g and 1h show the calculated minimum electron resonant energy for the first-order cyclotron resonance with parallel-propagating right-hand polarized waves at a frequency of 40 Hz (magenta line in Figure 1b). As shown in Figure 1g, the minimum resonant energy captures the main energy of injected electrons. Figure 1i shows the electron pitch angle distribution at 54 keV which exhibits a pronounced modulation. The vertical dashed lines present the minima of the electron fluxes at 54 keV. Figure 1d illustrates the convective linear growth rates for parallel-propagating whistler mode waves that were calculated using the electron distribution measured by MagEIS based on the equations of *Summers et al.* [2009]. The modulation of linear growth rate appears to correlate well with the observed hiss wave spectral intensity with a period of several minutes.

Changes in the background magnetic field, plasma density and the injected electron distribution (flux and pitch angle anisotropy of resonant electrons) could potentially be responsible for the hiss wave growth. Since the variation of the background magnetic field is small (~ 4 nT) compared to the median value (~ 150 nT), the effect of background magnetic field on the wave growth rate is likely to be insignificant compared to the effects of plasma density and electron injection. To distinguish the roles of these two effects in the local wave amplification, we compared the hiss wave amplitude with spin averaged electron flux and plasma density. The hiss wave amplitude integrated from 20 Hz to 1000 Hz is shown in Figure 2a. Figure 2b presents the spin averaged electron flux integrated

over the energy range from 30 keV to 200 keV. The vertical dashed lines in Figure 2 depict the same times as in Figure 1.

Figure 2c shows the comparison between the filtered electron flux (black) over 1.5 mHz - 4 mHz and the filtered hiss wave intensity (blue) over 1.5 mHz - 4 mHz. It suggests that the hiss intensity is well correlated with the variation of the electron flux. The correlation coefficient between the filtered electron flux and the filtered hiss wave intensity in the time period from 20:00 UT to 22:00 UT is 0.841. The satellite was located at a magnetic latitude of $-1.3^{\circ} \sim -2.0^{\circ}$, which was near the source region where local wave amplification typically occurs, and this is probably why hiss intensity and electron flux exhibit a remarkable correlation.

In the present hiss modulation event, the filtered background plasma density (green line in Figure 2d) is not well correlated with the filtered wave intensity (with a correlation coefficient of 0.105), especially during the period from 20:45 UT to 21:40 UT. This suggests that the variation of plasma density plays an insignificant role in the modulation of hiss wave intensity during this event. To investigate the sole effect of density on hiss intensity, we also calculated the correlation coefficient between the non-filtered hiss wave intensity and non-filtered the plasma density which even shows a slight anti-correlation with a coefficient of ~ -0.483 .

The comparison between the filtered electron pitch angle anisotropy at 54 keV and filtered wave intensity is shown in Figure 2e. Although a correlation coefficient of 0.378 indicates a certain correlation between these two parameters, it is much lower than the

correlation between the hiss wave intensity and electron flux (0.841). Therefore, we suggest that the variation of electron pitch angle anisotropy play a less important role in hiss intensity modulation compared to the variation of electron flux.

The electron flux variation observed by Van Allen Probe B may be caused by ULF wave modulation since they have similar time periods. Figure 3 shows the variation of electron fluxes at different energy channels observed by both Van Allen Probe A (a) and Van Allen Probe B (b). At $\sim 19:30$ UT, both probes, especially Van Allen Probe B observed intense electron injections. Between 20:00 and 22:00 UT, the energetic electron fluxes observed by Probe B are modulated at most energy channels, with a time period of several minutes in the same frequency range as typical ULF waves (Pc4-5).

Figure 4 is the summary of the Pc4-5 ULF waves from Van Allen Probe B during the time interval of interest (20:00–22:00 UT). Dynamic spectrograms of the ULF wave powers are shown for the three components of the magnetic field (in the mean field-aligned, geocentric solar magnetospheric (GSM) coordinates) along with the y component of the electric field in modified geocentric solar elliptic (MGSE) coordinate. Band-pass filtered time series (1.5-4 mHz) are shown below for each dynamic spectrogram. The parallel magnetic field (B_{para}) and y component electric field in MGSE coordinate (E_y) have a similar frequency peak at ~ 2.6 mHz. The wave spectra of the E_y and B_{para} components suggest that the compressional mode and shear mode are likely coupled.

The correlation of the ULF waves and the energetic electron fluxes at different energy channels is shown in Figure 5. Figure 5a illustrates the filtered E_y component of the electric

field between 1.5 and 4 mHz. Since Van Allen Probe B is near noon, the E_y component approximately represents the electric field in the azimuthal direction. Band-pass filtered electron fluxes normalized by unperturbed levels at different energy channels are shown in Figure 5b. The vertical black lines indicate the minima of the E_y component. The electron fluxes at various energies show a modulation period which is very similar to that of E_y . Besides, these fluxes exhibit an energy-dependent phase shift with respect to E_y . The phase of the electron flux oscillations with respect to E_y is closest to 180° out-of-phase at ~ 466 keV. At lower energies, the phase of peak electron fluxes relative to the E_y minimum varies but is not 180° out-of-phase. For the observed modulating hiss, the minimum resonant energy is tens of keV (Figure 1), and thus the electron flux at energy below 100 keV plays a dominant role in hiss amplification. Although these low energy electrons (30–100 keV) are not exactly in drift resonance with the observed ULF waves, their modulation is highly relevant to the presence of ULF waves. These low energy electrons may be accelerated by the ULF waves during the first half cycle and then decelerated so that there is no total energy gain. This mechanism was also demonstrated in the drift-resonance theory in which the peak electron fluxes should have a 180° energy shift [*Southwood and Kivelson, 1981*].

Meanwhile, Van Allen Probe A detected hiss emissions in a similar frequency range as shown in Figure 6. During this time period, Van Allen Probe A was located at lower L shells ($2.6 < L < 5.3$) and later MLTs ($14.9 < \text{MLT} < 18.0$). The hiss intensity also exhibited modulation in electric and magnetic field, as shown in Figures 6b and 6c, respectively. However, different from the observation by Probe B, the hiss intensity is dominantly

modulated by the variation of the plasma density. Figure 6d shows the density profile obtained from EMFISIS (black) and EFW (red). Examples of evident modulations by variation of plasma density are highlighted with grey blocks. According to ray tracing simulation [Chen *et al.*, 2012c], the hiss waves tend to propagate to the region with higher density resulting in higher wave intensity. Figures 6e and 6f show the spin averaged electron flux and pitch angle anisotropy based on MagEIS data and the white lines are the minimum resonant energy corresponding to a frequency of 40 Hz (Figure 6b). There is no clear correlation between the hiss intensity and electron flux, suggesting that the modulations are mainly caused by the plasma density variation. We also calculated the convective linear growth rates for parallel-propagating whistler mode waves as shown in Figure 6g. The growth rate profile shows little correlation with that of the observed hiss intensity, indicating that these waves are not locally excited.

Figure 7 illustrates the comparison of hiss wave frequency spectra observed by Van Allen Probes A (Figures 7a-7b) and B (Figures 7c-7d). At the beginning of the emission around 20:20 UT, the hiss wave intensity as a function of frequency observed by Van Allen Probe A presents a minimum at ~ 200 Hz (indicated by the white arrows in Figures 7a and 7b). This feature is similar to the observation by Van Allen Probe B (Figures 7c and 7d), where the modulation of hiss wave power below 100 Hz is correlated with the calculated wave growth rate (Figure 1d) based on the observed electron distribution. The hiss wave frequency spectra and structures observed by Probe A are similar to those observed by Probe B, but the energy spectra of energetic electrons are significantly different. Therefore,

the hiss emission observed by Probe A may be the result of wave propagation from the source region in the outer plasmasphere and further modulated by the local plasma density variation.

4. Summary and Discussion

We report clear evidence of local amplification of plasmaspheric hiss observed by Van Allen Probe B in the postnoon sector of the outer plasmaphere. The minimum resonance energy calculated for the observed hiss wave frequency is consistent with the energy of injected electrons. The hiss wave intensity was modulated by the injected energetic electrons, which were modulated by ULF waves. In the meantime, Van Allen Probe A also observed similar hiss emissions at lower L shells, which is probably due to the propagation from the source region in the outer plasmasphere. Different from the observation by Probe B, the hiss wave intensity observed by Probe A is predominantly affected by the background plasma density. The modulation of hiss intensity by plasma density could be due to the effect of ray focusing at high-density region during propagation [Chen *et al.*, 2012c].

Figure 8 summarizes the processes discussed in this study. The injected energetic electrons with energies of tens to hundreds of keV drift from the nightside to the dayside in the outer plasmasphere. Simultaneously, the ULF waves modulate the energetic electron fluxes. The modulated energetic electrons then lead to the modulation of the hiss intensity via local amplification. These features were all well captured by Van Allen Probe B. During

the same time period, Probe A at a later MLT and lower L shell observed hiss emissions which may originate from the source region in the outer plasmasphere.

Chorus waves which are intense coherent electromagnetic emissions exhibiting discrete rising or falling tones are believed to be generated through cyclotron resonance with anisotropic electrons [Kennel and Petschek, 1966; Anderson and Maeda, 1977; Meredith *et al.*, 2001; Li *et al.*, 2009]. It has been shown that ULF waves can modulate chorus intensity by modulating the background magnetic field and/or plasma density which affect the number of energetic electrons resonant with chorus waves [Li *et al.*, 2011]. Besides, the ULF wave-induced modulation of chorus could have an impact on electron precipitation leading to pulsating aurora [Jaynes *et al.*, 2015]. Similar modulations may also be captured in hiss wave intensity if hiss is locally amplified. However, different from chorus, plasmaspheric hiss waves are commonly known to be structureless [Thorne *et al.*, 1973] and wave propagation is believed to be important for the measured hiss wave intensification [Bortnik *et al.*, 2008, 2009; Chen *et al.*, 2014]. The hiss wave intensity is typically modulated by the variation of the background plasma density [Chen *et al.*, 2012c]. Nonetheless, our study showed the first evidence of the hiss wave modulation caused by modulated injected electrons due to ULF waves, clearly indicating that the hiss is locally amplified in the outer plasmasphere. It also provides an interesting link between the ULF waves and hiss waves which are in two distinct frequency ranges but both play important roles in radiation belt electron dynamics.

Acknowledgments

The work at Boston University is supported by the NASA grants NNX15AI96G, NNX17AG07G, and NNX17AD15G and the NSF grant AGS-1723342. The research at the University of Minnesota was supported by JHU/APL contract UMN 922613 under NASA contract JHU/APL NAS5-01072. We acknowledge the RBSP-ECT and EMFISIS funding provided by JHU/APL contract No. 967399 and 921647 under NASA's prime contract No. NAS5-01072. We would like to thank Dr. Lei Dai and Dr. Xu-Zhi Zhou for very helpful discussions in this study. We would like to acknowledge the EMFISIS data obtained from <http://emfisis.physics.uiowa.edu>, the MagEIS data obtained from <http://www.rbsp-ect.lanl.gov/science/DataDirectories.php>, and the EFW data obtained from <http://rbsp.space.umn.edu/data/rbsp/>. We also thank the World Data Center for Geomagnetism, Kyoto for providing AE index used in this study.

References

- Albert, J. M. (2005), Evaluation of quasi-linear diffusion coefficients for whistler mode waves in a plasma with arbitrary density ratio, *J. Geophys. Res.*, *110*, A03218, doi:10.1029/2004JA010844.
- Anderson, R. R., and K. Maeda (1977), VLF emissions associated with enhanced magnetospheric electrons, *J. Geophys. Res.*, *82*(1), 135–146, doi:10.1029/JA082i001p00135.
- Blake, J. B., et al. (2013), The Magnetic Electron Ion Spectrometer (MagEIS) Instruments Aboard the Radiation Belt Storm Probes (RBSP) spacecraft, *Space. Sci. Rev.*, doi:10.1007/s11214-013-9991-8.
- Bortnik, J., R. M. Thorne, and N. P. Meredith (2008), The unexpected origin of plasmaspheric hiss from discrete chorus emissions, *Nature*, *452*, 62–66, doi:10.1038/nature06741.
- Bortnik, J., W. Li, R. M. Thorne, V. Angelopoulos, C. Cully, J. Bonnell, O. Le Contel, and A. Roux (2009), An Observation linking the origin of plasmaspheric hiss to discrete chorus emissions, *Science*, *324*, 775–778, doi:10.1126/science.1171273.
- Breneman, A. W., et al. (2015), Global-scale coherence modulation of radiation-belt electron loss from plasmaspheric hiss, *Nature*, *523*, 193–195, doi:10.1038/nature14515.
- Chen, M. W., J. L. Roeder, J. F. Fennell, L. R. Lyons, R. L. Lambour, and M. Schulz (1999), Proton ring current pitch angle distributions: Comparison of simulations with CRRES observations, *J. Geophys. Res.*, *104*(A8), 17,379–17,389.

-
- 314 Chen, L., J. Bortnik, W. Li, R. M. Thorne, and R. B. Horne (2012a), Modeling the
315 properties of plasmaspheric hiss: 1. Dependence on chorus wave emission, *J. Geophys.*
316 *Res.*, *117*, A05201, doi:10.1029/2011JA017201.
- 317 Chen, L., J. Bortnik, W. Li, R.M. Thorne, and R. B. Horne (2012b), Modeling the
318 properties of plasmaspheric hiss: 2. Dependence on the plasma density distribution, *J.*
319 *Geophys. Res.*, *117*, A05202, doi:10.1029/2011JA017202.
- 320 Chen, L., R. M. Thorne, W. Li, J. Bortnik, D. Turner, and V. Angelopoulos (2012c),
321 Modulation of plasmaspheric hiss intensity by thermal plasma density structure,
322 *Geophys. Res. Lett.*, *39*, L14103, doi:10.1029/2012GL052308.
- 323 Chen, L., et al. (2014), Generation of unusually low frequency plasmaspheric hiss, *Geophys.*
324 *Res. Lett.*, *41*, 5702–5709, doi:10.1002/2014GL060628.
- 325 Chen, X.-R., Q.-G. Zong, X.-Z. Zhou, J. B. Blake, J. R. Wygant, and C. A.
326 Kletzing (2016), Van allen probes observation of a 360° phase shift in the flux
327 modulation of injected electrons by ULF waves, *Geophys. Res. Lett.*, *44*, 1614–1624,
328 doi:10.1002/2016GL071252.
- 329 Church, S. R., and R. M. Thorne (1983), On the origin of plasmaspheric hiss—Raypath
330 integrated amplification, *J. Geophys. Res.*, *88*, 7941–7957,
331 doi:10.1029/JA088iA10p07941.
- 332 Huang, C. Y., C. K. Goertz, and R. R. Anderson (1983), A theoretial study of plasmaspheric
333 hiss generation, *J. Geophys. Res.*, *88*, 7927–7940, doi:10.1029/JA088iA10p07927.

-
- 334 Claudepierre, S. G., et al. (2013), Van Allen Probes observation of localized drift resonance
335 between poloidal mode ultra-low frequency waves and 60 keV electrons, *Geophys. Res.*
336 *Lett.*, *40*, 4491–4497, doi:10.1002/grl.50901.
- 337 Dai, L., et al. (2013), Excitation of poloidal standing Alfvén waves through drift resonance
338 wave-particle interaction, *Geophys. Res. Lett.*, *40*, 4127–4132, doi:10.1002/grl.50800.
- 339 Green, J. L., S. Boardsen, L. Garcia, W. W. L. Taylor, S. F. Fung, and B. W. Reinisch
340 (2005), On the origin of whistler mode radiation in the plasmasphere, *J. Geophys. Res.*,
341 *110*, A03201, doi:10.1029/2004JA010495.
- 342 Hao, Y. X., et al. (2014), Interactions of energetic electrons with ULF waves triggered by
343 interplanetary shock: Van Allen Probes observations in the magnetotail, *J. Geophys.*
344 *Res. Space Physics*, *119*, 8262–8273, doi:10.1002/2014JA020023.
- 345 Jaynes, A. N., et al. (2015), Correlated Pc4–5 ULF waves, whistler-mode chorus, and
346 pulsating aurora observed by the Van Allen Probes and ground-based systems, *J.*
347 *Geophys. Res. Space Physics*, *120*, 8749–8761, doi:10.1002/2015JA021380.
- 348 Kennel, C. F., and H. E. Petschek (1966), Limit on stably trapped particle fluxes, *J.*
349 *Geophys. Res.*, *71*(1), 1–28, doi:10.1029/JZ071i001p00001.
- 350 Kletzing, C. A., et al. (2013), The Electric and Magnetic Field Instrument Suite and
351 Integrated Science (EMFISIS) on RBSP, *Space Sci. Rev.*, *179*, 127–181,
352 doi:10.1007/s11214-013-9993-6.
- 353 Kurth, W. S., De Pascuale, S., Faden, J. B., Kletzing, C. A., Hospodarsky, G. B., Thaller,
354 S. and Wygant, J. R. (2015), Electron densities inferred from plasma wave spectra

-
- 355 obtained by the Waves instrument on Van Allen Probes. *J. Geophys. Res. Space*
356 *Physics*, 120: 904–914. doi: 10.1002/2014JA020857.
- 357 Li, L., X.-Z. Zhou, Q.-G. Zong, R. Rankin, H. Zou, Y. Liu, X.-R. Chen, and Y.-X.
358 Hao (2017), Charged particle behavior in localized ultralow frequency waves: Theory
359 and observations, *Geophys. Res. Lett.*, 44, 5900–5908, doi:10.1002/2017GL073392.
- 360 Li, W., R. M. Thorne, V. Angelopoulos, J. W. Bonnell, J. P. McFadden, C. W. Carlson, O.
361 LeContel, A. Roux, K. H. Glassmeier, and H. U. Auster (2009), Evaluation of whistler-
362 mode chorus intensification on the nightside during an injection event observed on the
363 THEMIS spacecraft, *J. Geophys. Res.*, 114, A00C14, doi:10.1029/2008JA013554.
- 364 Li, W., R. M. Thorne, J. Bortnik, Y. Nishimura, and V. Angelopoulos (2011), Modulation
365 of whistler mode chorus waves: 1. Role of compressional Pc4–5 pulsations, *J. Geophys.*
366 *Res.*, 116, A06205, doi:10.1029/2010JA016312.
- 367 Li, W., et al. (2013), An unusual enhancement of low-frequency plasmaspheric hiss in the
368 outer plasmasphere associated with substorm-injected electrons, *Geophys. Res. Lett.*,
369 40, 3798–3803, doi:10.1002/grl.50787.
- 370 Li, W., Q. Ma, R. M. Thorne, J. Bortnik, C. A. Kletzing, W. S. Kurth, G. B. Hospodarsky,
371 and Y. Nishimura (2015a), Statistical properties of plasmaspheric hiss derived from
372 Van Allen Probes data and their effects on radiation belt electron dynamics. *J. Geophys.*
373 *Res. Space Physics*, 120, 3393–3405. doi: 10.1002/2015JA021048.
- 374 Li, W., L. Chen, J. Bortnik, R. M. Thorne, V. Angelopoulos, C. A. Kletzing, W. S. Kurth,
375 and G. B. Hospodarsky (2015b), First evidence for chorus at a large geocentric distance

-
- 376 as a source of plasmaspheric hiss: Coordinated THEMIS and Van Allen Probes
377 observation, *Geophys. Res. Lett.*, 42, 241–248, doi:10.1002/2014GL062832.
- 378 Lyons, L. R., R. M. Thorne, and C. F. Kennel (1972), Pitch-angle diffusion of radiation
379 belt electrons within the plasmasphere, *J. Geophys. Res.*, 77(19), 3455–3474,
380 doi:10.1029/JA077i019p03455.
- 381 Lyons, L. R., and R. M. Thorne (1973), Equilibrium structure of radiation belt electrons, *J.*
382 *Geophys. Res.*, 78(13), 2142–2149, doi:10.1029/JA078i013p02142.
- 383 Ma, Q., et al. (2016), Characteristic energy range of electron scattering due to
384 plasmaspheric hiss, *J. Geophys. Res. Space Physics*, 121, 11,737–11,749,
385 doi:10.1002/2016JA023311.
- 386 Mauk, B. H., N. J. Fox, S. G. Kanekal, R. L. Kessel, D. G. Sibeck, and A. Ukhorskiy (2012),
387 Science Objectives and Rationale for the Radiation Belt Storm Probes Mission, *Space*
388 *Sci. Rev.*, 1–15, doi:10.1007/s11214-012-9908-y.
- 389 Meredith, N. P., R. B. Horne, and R. R. Anderson (2001), Substorm dependence of chorus
390 amplitudes: Implications for the acceleration of electrons to relativistic energies, *J.*
391 *Geophys. Res.*, 106(A7), 13,165–13,178, doi:10.1029/2000JA900156.
- 392 Meredith, N. P., R. B. Horne, M. A. Clilverd, D. Horsfall, R. M. Thorne, and R. R.
393 Anderson (2006), Origins of plasmaspheric hiss, *J. Geophys. Res.*, 111, A09217,
394 doi:10.1029/2006JA011707.

-
- 395 Meredith, N.P., Horne, R. B., Glauert, S. A., & Anderson, R. R. (2007), Slot region electron
396 loss timescales due to plasmaspheric hiss and lightning generated whistlers, *Journal of*
397 *Geophysical Research*, 112, A08214, doi:10.1029/2006JA012413
- 398 Meredith, N. P., Horne, R. B., Glauert, S. A., Baker, D. N., Kanekal, S. G., & Albert, J.M.
399 (2009), Relativistic electron loss timescales in the slot region, *Journal of Geophysical*
400 *Research*, 114, A03222, doi:10.1029/2008JA013889
- 401 Meredith, N. P., R. B. Horne, J. Bortnik, R. M. Thorne, L. Chen, W. Li, and A. Sicard-
402 Piet (2013), Global statistical evidence for chorus as the embryonic source of
403 plasmaspheric hiss, *Geophys. Res. Lett.*, 40, 2891-2896, doi:10.1002/grl.50593.
- 404 Ni, B., J. Bortnik, R. M. Thorne, Q. Ma, and L. Chen (2013), Resonant scattering and
405 resultant pitch angle evolution of relativistic electrons by plasmaspheric hiss, *J.*
406 *Geophys. Res. Space Physics*, 118, 7740–7751, doi:10.1002/2013JA019260.
- 407 Ni, B., et al. (2014), Resonant scattering of energetic electrons by unusual low-frequency
408 hiss, *Geophys. Res. Lett.*, 40, 3798–3803, doi:10.1002/grl.50787.
- 409 Shi, R., Li, W., Ma, Q., Reeves, G. D., Kletzing, C. A., Kurth, W. S., ... Claudepierre, S.
410 G. (2017). Systematic evaluation of low-frequency hiss and energetic electron
411 injections. *Journal of Geophysical Research: Space Physics*, 122, 10,263–
412 10,274. <https://doi.org/10.1002/2017JA024571>.
- 413 Southwood, D. J., and M. G. Kivelson (1981), Charged particle behavior in low-frequency
414 geomagnetic pulsations. I Transverse waves, *J. Geophys. Res.*, 86, 5643–5655,
415 doi:10.1029/JA086iA07p05643.

-
- 416 Spence, H. E., et al. (2013), Science Goals and Overview of the Energetic Particle,
 417 Composition, and Thermal Plasma (ECT) Suite on NASA's Radiation Belt Storm
 418 Probes (RBSP) Mission, *Space Sci. Rev.*, doi:10.1007/s11214-013-0007-5.
- 419 Summers, D., B. Ni, N. P. Meredith, R. B. Horne, R. M. Thorne, M. B. Moldwin, and R.
 420 R. Anderson (2008), Electron scattering by whistler-mode ELF hiss in plasmaspheric
 421 plumes, *J. Geophys. Res.*, *113*, A04219, doi:10.1029/2007JA012678.
- 422 Summers, D., R. Tang, and R. M. Thorne (2009), Limit on stably trapped particle fluxes in
 423 planetary magnetospheres, *J. Geophys. Res.*, *114*, A10210, doi:10.1029/2009JA014428.
- 424 Thorne, R. M., E. J. Smith, R. K. Burton, and R. E. Holzer (1973), Plasmaspheric hiss, *J.*
 425 *Geophys. Res.*, *78*(10), 1581–1596, doi:10.1029/JA078i010p01581.
- 426 Thorne, R. M., S. R. Church, and D. J. Gorney (1979), On the origin of plasmaspheric
 427 hiss—The importance of wave propagation and the plasmopause, *J. Geophys. Res.*, *84*,
 428 5241–5247, doi:10.1029/JA084iA09p05241.
- 429 Wang, C., Q. Zong, F. Xiao, Z. Su, Y. Wang, and C. Yue (2011), The relations between
 430 magnetospheric chorus and hiss inside and outside the plasmasphere boundary layer:
 431 Cluster observation, *J. Geophys. Res.*, *116*, A07221, doi:10.1029/2010JA016240.
- 432 Wygant J. R. et al. (2013), The Electric Field and Waves Instruments on the Radiation Belt
 433 Storm Probes Mission, *Space Science Reviews*, *179*, (1-4), pp.183-220,
 434 doi: 10.1007/s11214-013-0013-7.
- 435 Zhou, X.-Z., Z.-H. Wang, Q.-G. Zong, S. G. Claudepierre, I. R. Mann, M. G. Kivelson, V.
 436 Angelopoulos, Y.-X. Hao, Y.-F. Wang, and Z.-Y. Pu (2015), Imprints of impulse-

437 excited hydromagnetic waves on electrons in the Van Allen radiation belts, *Geophys.*
438 *Res. Lett.*, *42*, 6199–6204, doi:10.1002/2015GL064988.

439 Zhou, X.-Z., Z.-H. Wang, Q.-G. Zong, R. Rankin, M. G. Kivelson, X.-R. Chen, J. B.
440 Blake, J. R. Wygant, and C. A. Kletzing (2016), Charged particle behavior in the
441 growth and damping stages of ultralow frequency waves: Theory and Van Allen Probes
442 observations, *J. Geophys. Res. Space Physics*, *121*, 3254–3263,
443 doi:10.1002/2016JA022447.

444 Zong, Q.-G., et al. (2009), Energetic electron response to ULF waves induced by
445 interplanetary shocks in the outer radiation belt, *J. Geophys. Res.*, *114*, A10204,
446 doi:10.1029/2009JA014393.

Figure Captions

Figure 1. Plasmaspheric hiss modulation caused by injected electrons observed by Van Allen Probe B from 20:00 UT to 22:00 UT on January 12, 2014. (a) AE index; frequency-time spectrogram of (b) wave electric field and (c) wave magnetic field spectral density in the WFR channel; (d) frequency spectrum of convective linear wave growth rates; (e) background magnetic field intensity; (f) calibrated plasma density based on EFW and EMFISIS; (g) spin-averaged electron flux measured by MagEIS; (h) electron pitch angle anisotropy; (i) pitch angle distribution of electrons at 54 keV. The white dash-dotted line in Figure 1b represents the lower hybrid resonance frequency (f_{LHR}). The magenta line in Figure 1b indicates 40 Hz. The white dashed line in Figure 1c indicates 100 Hz. The black lines in Figures 1g and 1h represent the minimum resonant energy of electrons interacting with the waves at 40 Hz. The dashed vertical lines mark the modulation of the electron flux at 54 keV (Figure 1i).

Figure 2. (a) Integrated hiss intensity from 20 Hz to 1000 Hz; (b) integrated spin-averaged electron flux from 30 keV to 200 keV; (c) filtered integrated electron number flux (black) and filtered magnetic wave intensity of hiss (blue); (d) filtered plasma density (green) and filtered magnetic wave intensity of hiss (blue); (e) filtered pitch angle anisotropy (red) and filtered magnetic wave intensity of hiss (blue). The vertical dashed lines depict the same times as those in Figure 1.

Figure 3. Variation of electron fluxes at different energies observed by Van Allen Probe A (a) and Van Allen Probe B (b). In Figure 3b, the modulation of electron fluxes was

observed by Van Allen Probe B between 20:00:00 and 22:00:00 UT in association with ULF waves, and the dispersed electron injection was observed at ~19:30:00 UT.

Figure 4. Summary of the Pc4-5 ULF wave frequency spectra from Van Allen Probe B during the time interval of interest (20:00-22:00 UT). Dynamic spectrograms are shown for the three components of the magnetic field (in the mean field-aligned, GSM coordinates) along with the y component of the electric field in MGSE coordinate. Band-pass filtered time series (1.5 - 4 mHz) are shown below for each dynamic spectrogram. The black dashed lines indicate the frequency at ~2.6 mHz.

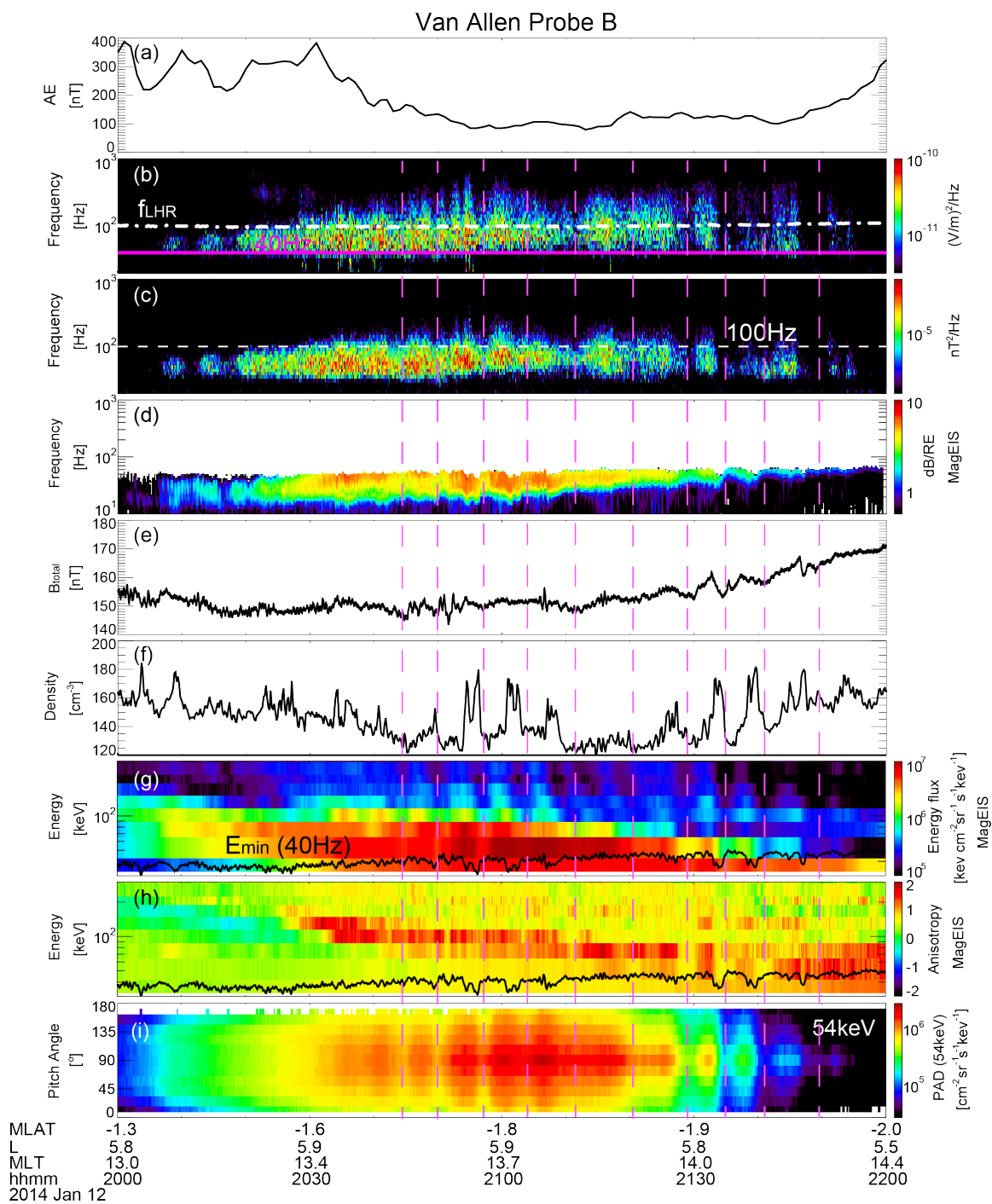
Figure 5. The correlation of the filtered (1.5 - 4 mHz) E_y component of ULF waves (a) and the energetic electron fluxes at different energy channels (b). The electron fluxes show the modulation in the similar period to that of E_y , but exhibit an energy-dependent phase shift with respect to E_y .

Figure 6. The observation of waves and electron fluxes by Van Allen Probe A during the same period as that in Figure 1. a) AE index; (b) frequency-time spectrogram of wave electric field and (c) wave magnetic spectral density in the WFR channel; (d) plasma density obtained by EFW (red) and EMFISIS (black); (e) spin-averaged electron flux measured by MagEIS; (f) electron pitch angle anisotropy; (g) convective wave growth rates. Grey block areas indicate the intervals of hiss modulation by variation of plasma density. The magenta line in Figure 6b indicates 40 Hz. The black dashed line in Figure 6c indicates 100 Hz. The white lines in Figures 6e and 6f represent the minimum resonant energy of electrons for the waves at 40 Hz.

Figure 7. The wave electric (a) and magnetic (b) spectral density observed by Van Allen Probe A and the wave electric (c) and magnetic (d) spectral density from Van Allen Probe B. Note that at the beginning of the emissions around 20:20 UT, the hiss wave intensity as a function of frequency presents a minimum at ~ 200 Hz (white arrows) for the observations from both Van Allen Probes A and B.

Figure 8. A cartoon showing energetic electron trajectory (green), ULF waves (pink) and hiss intensity modulation (blue). Injected electrons from the nightside drift to the postnoon sector (green arrow) in the outer plasmasphere where they provide a source of free energy for hiss wave generation in the outer plasmasphere. During the period of electron injection, electrons are modulated by ULF waves (magenta), which lead to the modulation of hiss wave amplification (blue), as observed by Van Allen Probe B. The hiss waves are probably generated in the outer plasmasphere, and then propagate into lower L shells, as observed by Van Allen Probe A.

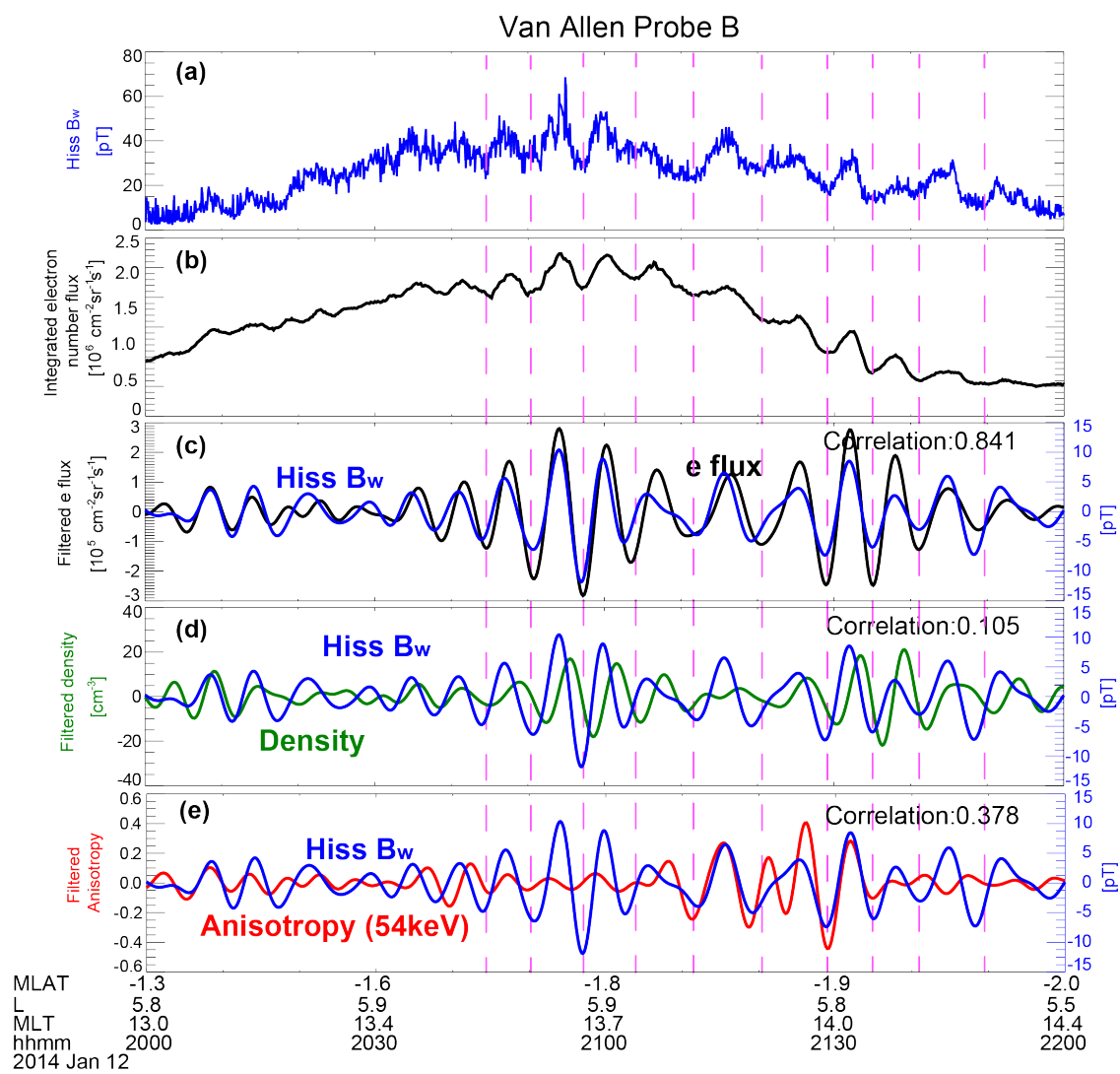
503 Figure 1



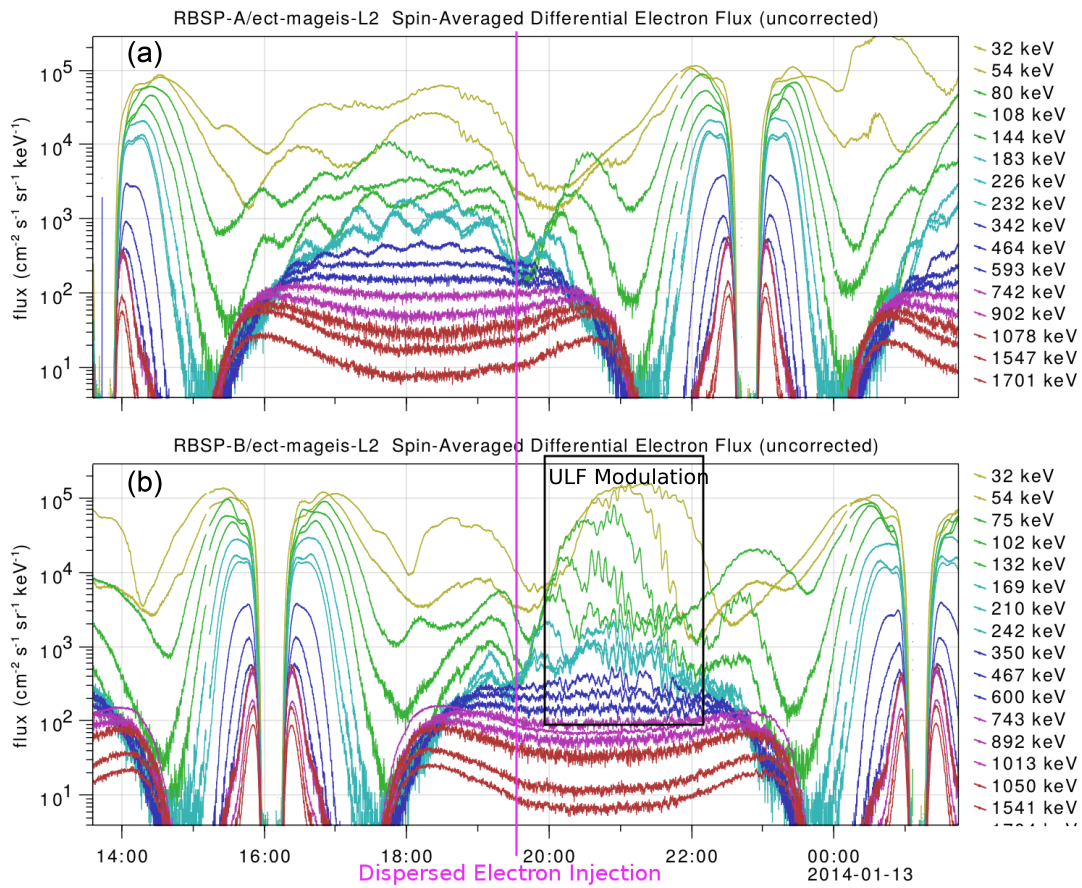
504

505

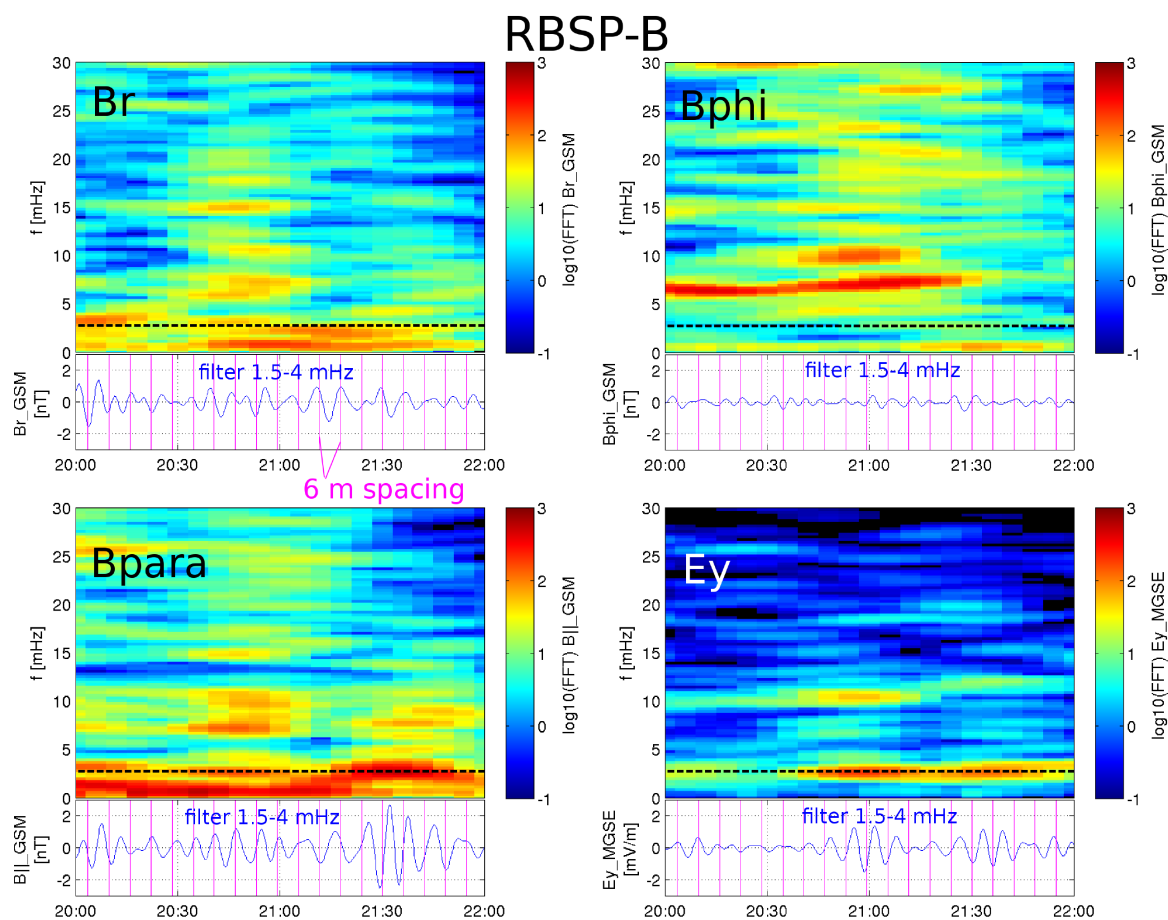
Figure 2



511 Figure 3.



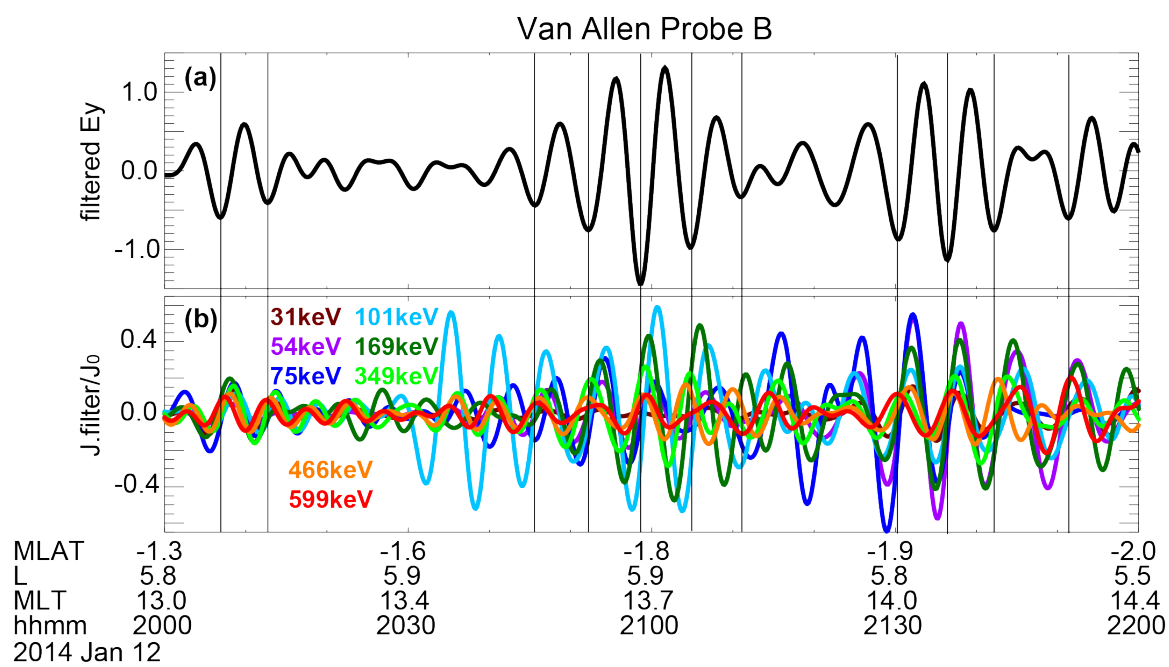
515 Figure 4



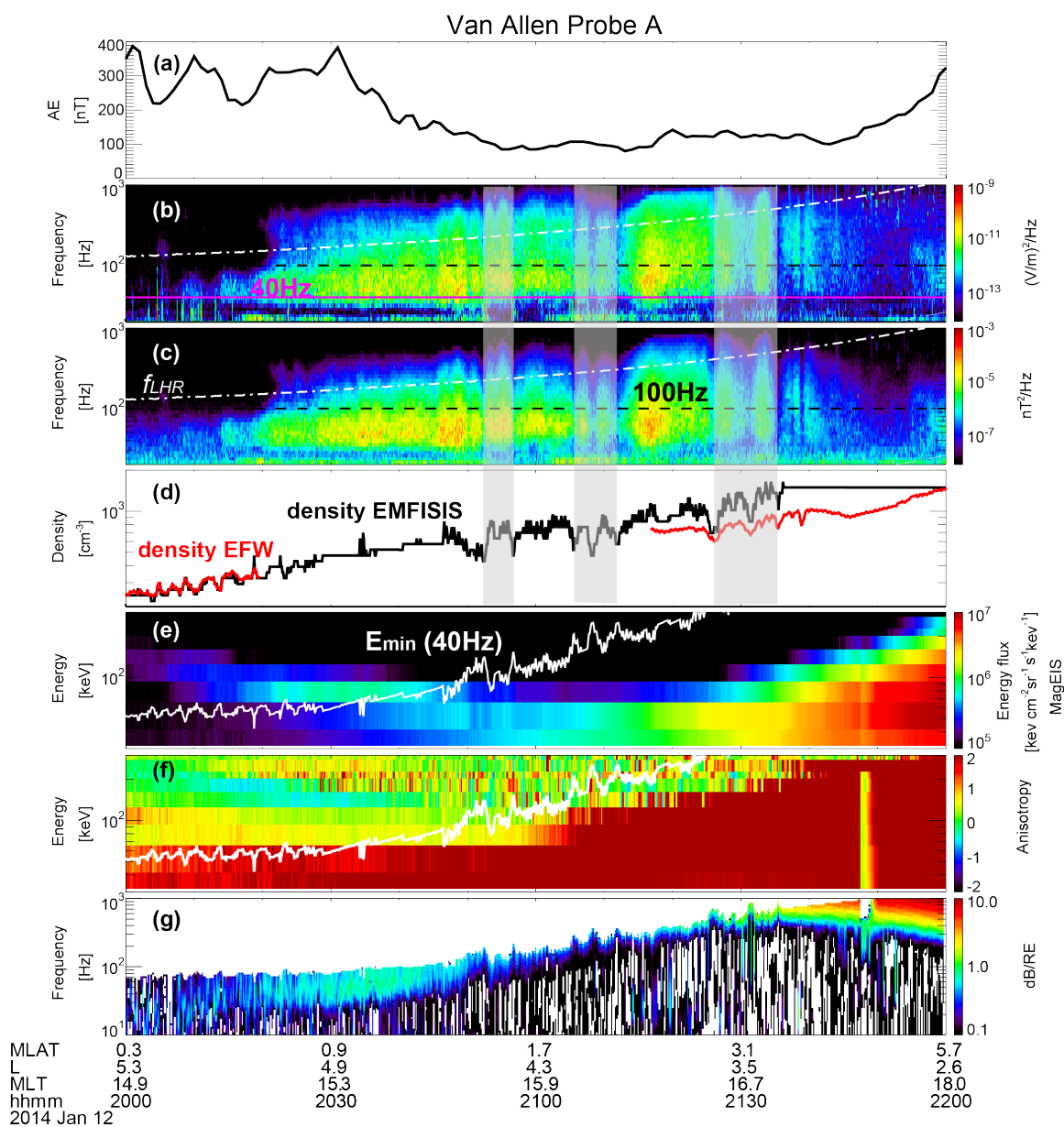
516

517

518 Figure 5



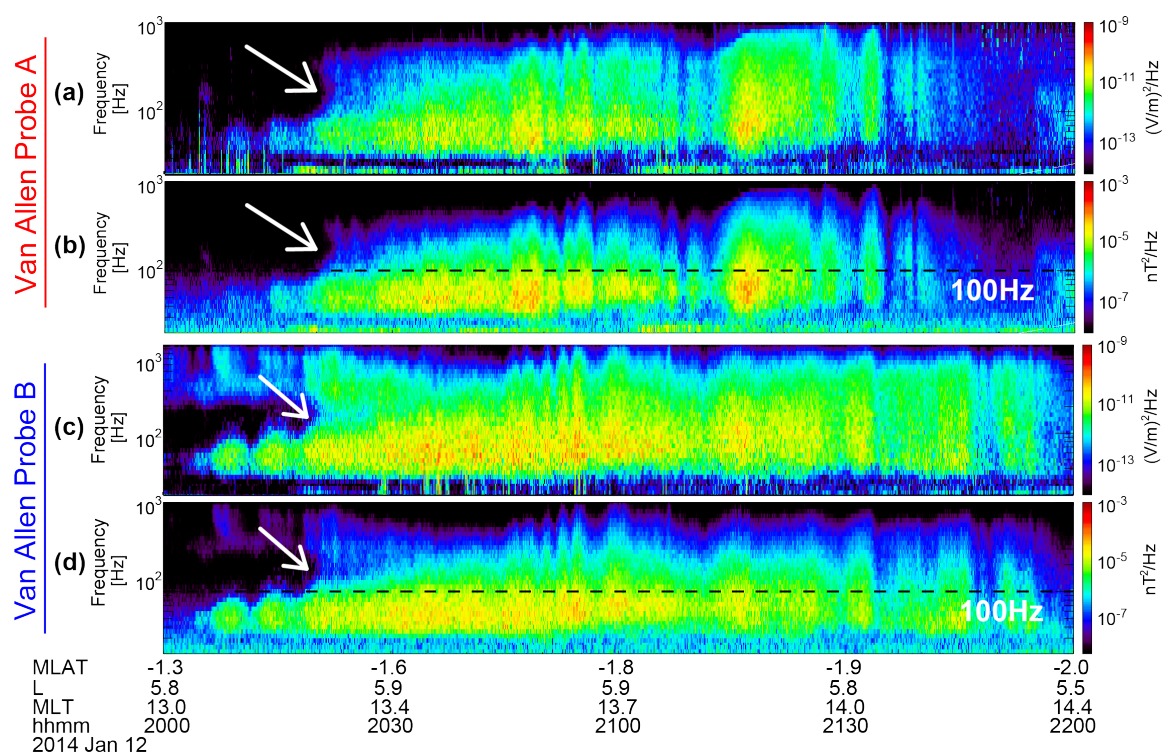
522 Figure 6



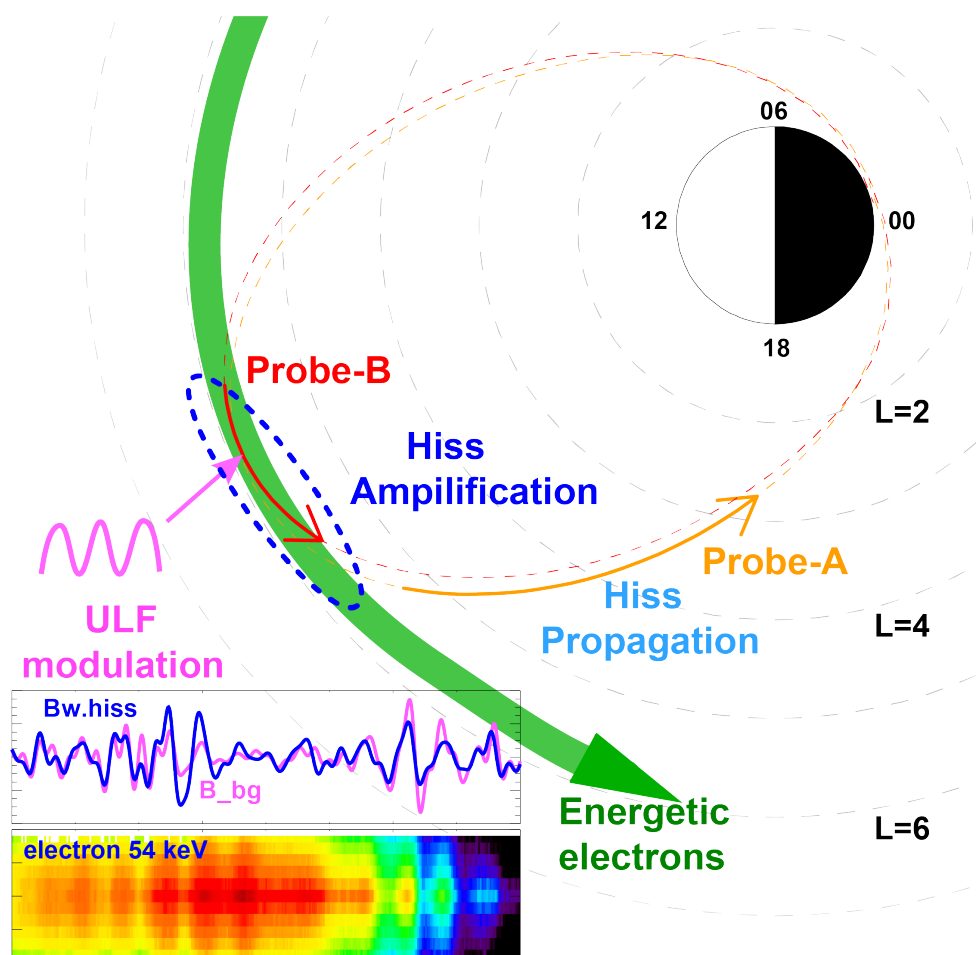
523

524

525 Figure 7



528 Figure 8



529